0026-895X/04/6603-478–491$20.00
MOLECULAR PHARMACOLOGY
Copyright © 2004 The American Society for Pharmacology and Experimental Therapeutics
Mol Pharmacol 66:478–491, 2004

Vol. 66, No. 3
3257/1172829
Printed in U.S.A.

DNA Damage Induced by Temozolomide Signals to both ATM and ATR: Role of the Mismatch Repair System

Simona Caporali, Sabrina Falcinelli, Giuseppe Starace, Maria Teresa Russo, Enzo Bonmassar, Josef Jiricny, and Stefania D'Atri

Istituto Dermopatico dell'Immacolata–Istituto di Ricovero e Cura a Carattere Scientifico, Rome, Italy (S.C., S.F., E.B., S.D.); Institute of Neurobiology and Molecular Medicine, National Research Council, Rome, Italy (G.S.); Section of Chemical Carcinogenesis, Istituto Superiore di Sanità, Rome, Italy (M.T.R.); and Institute of Molecular Cancer Research, University of Zürich, Zürich, Switzerland (J.J.)

Received February 5, 2004; accepted June 10, 2004

This article is available online at http://molpharm.aspetjournals.org

ABSTRACT

The mammalian mismatch repair (MMR) system has been implicated in activation of the G_2 checkpoint induced by methylating agents. In an attempt to identify the signaling events accompanying this phenomenon, we studied the response of MMR-proficient and -deficient cells to treatment with the methylating agent temozolomide (TMZ). At low TMZ concentrations, MMR-proficient cells were growth-inhibited, arrested in G_2/M, and proceeded to apoptosis after the second post-treatment cell cycle. These events were accompanied by activation of the ATM and ATR kinases, and phosphorylation of Chk1, Chk2, and p53. ATM was activated later than ATR and was dispensable for phosphorylation of Chk1, Chk2, and p53 on Ser15 and for triggering of the G_2/M arrest. However, it conferred protection against cell growth inhibition induced by TMZ. ATR was activated earlier than ATM and was required for an efficient phosphorylation of Chk1 and p53 on Ser15. Moreover, abrogation of ATR function attenuated the TMZ-induced G_2/M arrest and increased drug-induced cytotoxicity. Treatment of MMR-deficient cells with low TMZ concentrations failed to activate ATM and ATR and to cause phosphorylation of Chk1, Chk2, and p53, as well as G_2/M arrest and apoptosis. However, all these events occurred in MMR-deficient cells exposed to high TMZ concentrations, albeit with faster kinetics. These results demonstrate that TMZ treatment activates ATM- and ATR-dependent signaling pathways and that this process is absolutely dependent on functional MMR only at low drug concentrations.

Cell cycle checkpoints, signal transduction pathways activated in response to genotoxic stress, coordinate cell cycle progression with DNA repair and apoptosis to minimize the probability of replicating and segregating damaged DNA (reviewed in Zhou and Elledge, 2000). DNA damage-induced checkpoints act at the G_1-S phase transition, during the S phase, and at the G_2-M boundary. The serine/threonine protein kinases ATM (ataxia-telangiectasia mutated) and ATR (ATM and Rad3-related) are essential transducers of these checkpoints; in response to DNA damage, they phosphorylate numerous target proteins involved in cell cycle arrest, DNA repair, and apoptosis (reviewed in Abraham, 2001; Khanna et al., 2001; Shiloh, 2003). ATM is rapidly activated after exposure of cells to double-strand break-inducing agents such as ionizing radiation (IR). ATR is the principal signal transducer when cells are challenged with UV light or with agents that interfere with DNA replication and also enforces and sustains the checkpoints induced by DSBs (Abraham, 2001; Zhou et al., 2002; Shiloh, 2003).

Upon activation, ATM directly phosphorylates p53 on Ser15, whereas ATR phosphorylates it on Ser15 and Ser37 (Abraham, 2001; Khanna et al., 2001; Shiloh, 2003). ATM and ATR also phosphorylate Chk1 and Chk2 (Abraham, 2001; Khanna et al., 2001; Gatei et al., 2003; Shiloh, 2003), which in turn phosphorylate p53 on Ser20, and the Cdc25A and Cdc25C phosphatases on Ser123 and Ser216, respectively (Rhind and Russell, 2000; Bartek et al., 2001). Phos-

This study was supported by European Commission Grant QLG1-CT-2000-01230 and by the Italian Ministry of Health.

ABBREVIATIONS: ATM, ataxia-telangiectasia mutated; ATR, ataxia and Rad3-related; IR, ionizing radiation; MMR, mismatch repair; MNNG, *N*-methyl-*N′*-nitro-*N*-nitrosoguanidine; TMZ, temozolomide [8-carbamoyl-3-methyl-imidazo[5,1-*d*]-1,2,3,5-tetrazin-4(3H)-one]; O^6-MeG, O^6-methylguanine; MGMT, O^6-methylguanine-DNA methyltransferase; O^6-G, O^6-guanine; CM, complete medium; kd, kinase dead; BG, O^6-benzylguanine; zVAD-fmk, benzyloxycarbonyl-Val-Ala-DL-Asp(OMe)-fluoromethylketone; PBS, phosphate-buffered saline; AEBSF, 4-(2-aminoethyl)benzenesulfonyl fluoride; DTT, dithiothreitol; mAb, monoclonal antibody; PARP, poly(ADP-ribose) polymerase; zVAD-fmk, *N*-benzyloxycarbonyl-VAD-fluoromethyl ketone; PHAS-I, phosphorylated heat- and acid-stable protein regulated by insulin; DSB, double strand break; ECL, enhanced chemiluminescence.

phorylation of p53 on Ser15 and Ser20 contributes to the stabilization and functional activation of the protein, which plays a pivotal role in the G_1 checkpoint, participates in the G_2 checkpoint and promotes apoptosis (reviewed in Sionov and Haupt, 1999; Taylor and Stark, 2001). Phosphorylation of Cdc25A targets it for degradation. This event prevents the activation of the cyclin-dependent kinases Cdk2 and Cdc2, contributing to the G_1, S, and G_2 checkpoints (Rhind and Russell, 2000; Bartek et al., 2001). Phosphorylation of Cdc25C creates a binding site for 14-3-3 proteins, and the 14-3-3-bound form of Cdc25C is prevented from dephosphorylating and activating the mitotic cyclin B/Cdc2 kinase complex. The maintenance of the inhibitory phosphorylations on the cyclin B/Cdc2 kinase complex contributes to the G_2 checkpoint (Rhind and Russell, 2000; Bartek et al., 2001).

In addition to Chk1, Chk2, and p53, ATR and/or ATM phosphorylate a number of other target proteins, including BRCA1, NBS1, and SMC1 (Abraham, 2001; Khanna et al., 2001; Shiloh, 2003), which participate in DNA damage-induced checkpoints, although the underlying molecular mechanisms are less understood.

Several studies suggest that a functional mismatch repair (MMR) system (reviewed in Modrich, 1997; Jiricny and Nyström-Lahti, 2000) is required for a proper activation of cell cycle checkpoints in response to specific DNA damage (Kaina et al., 1997; D'Atri et al., 1998; Duckett et al., 1999; Hickman and Samson, 1999; Brown et al., 2003; Hirose et al., 2003; Wang and Qin, 2003).

In the case of methylating agents such as *N*-methyl-*N*′-nitro-*N*-nitrosoguanidine (MNNG), *N*-methyl-*N*-nitrosourea, and temozolomide (TMZ), it has been shown that MMR-deficient cells fail to stabilize p53 and phosphorylate it on Ser15 and Ser392. These cells fail to arrest at the G_2/M phase of the cell cycle and do not undergo apoptosis in response to drug concentrations that are highly effective in killing MMR-proficient cells (Kaina et al., 1997; D'Atri et al., 1998; Duckett et al., 1999; Hickman and Samson, 1999). Wang and Qin (2003) have also reported that abrogation of hMSH2 expression in HeLa cells leads to impaired phosphorylation of Chk1 and SMC1, and defective S-phase checkpoint activation after treatment with MNNG. Moreover, Hirose et al. (2003) have demonstrated that in response to TMZ, mitogen-activated protein kinase p38α is activated in MMR-proficient but not in MMR-deficient cells and that the protein is involved in drug-induced G_2/M arrest.

In cells exposed to TMZ, MNNG, and *N*-methyl-*N*-nitrosourea, cytotoxicity is mediated mainly by the formation of O^6-methylguanine (O^6-MeG) in DNA, because cells with high levels of the DNA-repair enzyme O^6-methylguanine-DNA methyltransferase (MGMT), which specifically removes alkyl adducts from the O^6 position of guanine (O^6-G), are more resistant to these drugs than MGMT-deficient cells (for review, see Pegg et al., 1995; Gerson, 2002). Because MMR-deficient cells are highly resistant to O^6-G-methylating agents, regardless of their MGMT activity, it has been proposed that cell cycle arrest and apoptosis induced by these drugs in MMR-proficient cells is triggered by MMR-mediated processing of O^6-MeG:T mispairs generated in the course of the first S-phase after treatment (for review, see Karran, 2001).

Although MMR-deficient cells are extremely resistant to O^6-MeG-generating agents, an impairment of proliferation occurs at high drug concentrations. It is reasonable to hypothesize that the generation of high levels of DNA damage distinct from O^6-MeG might account for cell growth inhibition.

The aim of the present study was to gain further insight into the signal transduction pathways activated as a consequence of MMR-mediated processing of O^6-MeG:T mispairs and to investigate whether MMR-deficient cells activate, in response to high concentrations of O^6-G-methylating agents, signal transduction pathways similar or different from those activated in MMR-proficient cells.

Materials and Methods

Cell Lines. The MMR-proficient human B lymphoblastoid cell lines TK6 (Kat et al., 1993) and its MMR-deficient subline MT1 (Kat et al., 1993; Papadopoulos et al., 1995) were maintained in RPMI-1640 medium (Hyclone Europe, Cramlington, UK) supplemented with 10% fetal calf serum (Hyclone Laboratories, Logan, UT), 2 mM L-glutamine, and 50 μg/ml gentamycin (Invitrogen, Paisley, UK) [referred to as complete medium (CM)]. Both lines are MGMT-deficient and thus fail to remove methyl adducts from O^6-G (Goldmacher et al., 1986). The MT1 cell line harbors a different missense mutation in both alleles of the *hMSH6* locus.

The KT MAT1 and KT MEP cell lines originated from the ataxia telangiectasia lymphoblastoid cell line KT through stable transfection with the $CdCl_2$-inducible ATM cDNA expression vector pMAT1 (KT MAT1 cells) or the empty vector pMEP (KT MEP cells) (Zhang et al., 1997). The cell lines were maintained in CM supplemented with 0.2 mg/ml hygromycin B (Roche Diagnostic GmbH, Mannheim, Germany). The expression of the ATM protein in KT MAT1 cells was achieved by treatment with 5 μM $CdCl_2$ (Sigma, St. Louis, MO) for 16 h (Zhang et al., 1997) and verified by Western blot analysis using a rabbit polyclonal antibody against ATM (NB 100–104; Novus Biologicals, Littleton, CO).

The U2OS (human osteosarcoma) cells stably transfected with a doxycycline-inducible, dominant-negative, kinase-dead ATR (ATR-kd) expression construct (Nghiem et al., 2001) were maintained in Dulbecco's modified Eagle's medium (Invitrogen), supplemented with 10% fetal calf serum, 0.2 mg/ml G418 (Sigma), and 50 μg/ml hygromycin B. Induction of ATR-kd in U2OS transfected cells was achieved by treatment with 1 μg/ml doxycycline (BD Biosciences Clontech, Palo Alto, CA) for 24 h (Nghiem et al., 2001).

Drugs and Reagents. TMZ was kindly provided by Schering-Plough Research Institute (Kenilworth, NJ). The MGMT inhibitor O^6-benzylguanine (BG) (Pegg et al., 1995) was purchased from Sigma. Benzyloxycarbonyl-Val-Ala-DL-Asp(OMe)-fluoromethylketone (zVAD-fmk) was obtained from Calbiochem (La Jolla, CA). TMZ was always prepared freshly in RPMI-1640, because the drug readily decomposes in aqueous solution. BG was dissolved in ethanol (2.4 mg/ml), and zVAD-fmk was dissolved in dimethyl sulfoxide (37.4 mg/ml). The two agents were stored as stock solutions at −80°C, and diluted in culture medium just before use. The final concentrations of ethanol or dimethyl sulfoxide did not affect cell growth (data not shown).

Cell Treatment and Cell Growth Evaluation. TK6 and MT1 cells were suspended (1×10^5 cells/ml) in CM or in CM containing the appropriate amount of TMZ and analyzed for cell growth after 12, 24, 36, 48, and 72 h of culture. For all the other analyses, untreated or drug-treated cells were collected at the indicated time points, washed in phosphate-buffered saline (PBS), and appropriately processed. Where indicated, TK6 cells were incubated in the presence of 200 μM zVAD-fmk for 2 h before the addition of TMZ.

KT MAT1 and KT MEP cells were cultured in CM containing 5 μM $CdCl_2$ for 16 h, washed, and suspended (1×10^5 cells/ml) in CM containing 10 μM BG. After a 2-h incubation, appropriate amounts of TMZ were added to the cultures, which were returned to the incu-

bator for additional 72 h. Control groups were treated only with $CdCl_2$ and BG. Cell growth was evaluated after 72 h of culture, whereas all the other analyses were performed at the indicated time points. KT MAT1 and KT MEP cells were exposed to 10 Gy of X-rays using the RADGIL irradiator (Gilardoni, Milan, Italy).

U2OS cells stably transfected with the doxycycline-inducible ATR-kd expression construct were cultured in the absence or in the presence of 1 μg/ml doxycycline for 24 h. TMZ (either 25 μM or 1.2 mM) and BG (10 μM) were then added to the cultures. BG was added to the cultures 2 h before TMZ. Control groups were treated only with BG or doxycycline plus BG. At the desired time points, control and TMZ-treated cells were harvested by trypsinization, washed in PBS, and appropriately processed for the analyses to be performed.

For cell growth evaluation, U2OS transfected cells were seeded (5×10^3 cells/well) into 24-well plates (Falcon; BD Biosciences Discovery Labware, Bedford, MA) and exposed to doxycycline (1 μg/ml), BG (10 μM), and TMZ (25 μM) as described above. Ninety-six hours after the addition of TMZ, the cells were harvested by trypsinization and counted by hemocytometer and trypan blue exclusion. Four replica wells were used for controls and drug-treated groups.

Cell Cycle and Apoptosis Analysis. Cells were fixed and stained with propidium iodide as described previously (D'Atri et al., 1998). The propidium iodide fluorescence was measured on a linear scale using a FACScan flow cytometer (BD Biosciences, San Jose, CA). Data were recorded using the CellQuest software (BD Biosciences) and analyzed by a mathematical model of the cell cycle (Bertuzzi et al., 1983). Apoptotic cells were determined by their hypochromic, sub-G_1 staining profiles.

Western Blot Analyses. Total cellular extracts were prepared by incubating cells on ice in lysis buffer (50 mM Tris-HCl, pH 7.4, 150 mM NaCl, 1 mM EGTA, 1% Nonidet P-40, 0.25% sodium deoxycholate, 1 mM NaF, 1 mM Na_3VO_4, 1 mM AEBSF) supplemented with 1× of a protease inhibitor cocktail (Complete EDTA-free; Roche Diagnostic) for 10 min. The cell lysates were then clarified by centrifugation, diluted in 5× Lämmli sample buffer, and boiled for 5 min. To analyze phosphorylation of p53, Chk1, and Chk2, the cells were lysed in SDS sample buffer (62.5 mM Tris-HCl, pH 6.8, 2% SDS, 10% glycerol, 50 mM DTT, and 0.01% bromphenol blue), sonicated, and then boiled. Samples were electrophoresed on SDS-polyacrylamide gels, transferred to nitrocellulose membranes (Amersham Biosciences, Buckinghamshire, UK), and blocked with 5% nonfat milk in Tris-buffered saline supplemented with 0.1% Tween 20 (TBST) for 1 h. The membranes were then incubated in the same solution overnight at 4°C with primary antibodies. After washing three times with TBST, the membranes were incubated with horseradish peroxidase-linked secondary antibodies (Amersham Biosciences) at room temperature for 1 h and washed again in TBST. Protein bands were then visualized using the ECL method (Amersham Biosciences).

Rabbit polyclonal antibodies against p53, phospho-p53 (Ser9), phospho-p53 (Ser15), phospho-p53 (Ser20), phospho-p53 (Ser37), phospho-p53 (Ser46), phospho-p53 (Ser392), phospho-Chk1 (Ser-345), and phospho-Chk2 (Thr68) were purchased from Cell Signaling Technology, Inc. (Beverly, MA). Rabbit polyclonal antibodies against Chk1 (FL-476) were obtained from Santa Cruz Biotechnology, Inc. (Santa Cruz, CA). Rabbit polyclonal antibodies against Chk2 were purchased from Upstate Biotechnology (Lake Placid, NY). The mouse monoclonal antibody (mAb) against actin (clone AC-40) and the anti-FLAG M2 mAb were obtained from Sigma. The mouse mAb against poly(ADP-ribose) polymerase (PARP) (clone C-2–10) was purchased from BD Biosciences Clontech and the mouse mAb against p21/waf1 (Clone 70) was from BD Transduction Laboratories (Lexington, CA).

ATM and ATR Kinase Assay. ATM and ATR were immunoprecipitated from cells as described by Ye et al. (2001) with minor modifications. In brief, 1×10^7 cells were collected, washed in PBS, suspended in 0.35 ml of immunoprecipitation buffer (50 mM Tris-HCl, pH 7.5, 50 mM β-glycerophosphate, 150 mM NaCl, 10% glycerol, 1% Tween 20, 1 mM NaF, 1 mM Na_3VO_4, 1 mM DTT, 1 mM AEBSF, and 1× protease inhibitor cocktail Complete EDTA-free) and lysed by sonication. The lysates were cleared by centrifugation, and the supernatants were subjected to preimmunoprecipitation with normal rabbit IgG and protein A/G-agarose beads (Santa Cruz Biotechnology) for 1 h, followed by immunoprecipitation with a rabbit polyclonal antibody against ATM (Ab3; Oncogene Science, Cambridge, MA) or ATR (Ab2; Oncogene) for 3 h. As a control, the immunoprecipitation was also performed with normal rabbit IgG. In preliminary experiments, the absence of cross-reactivity of the Ab3 and Ab2 antibodies with the ATR and ATM proteins, respectively, was verified by Western blot analysis. No ATR band was detected in ATM immunoprecipitates subjected to immunoblotting with the Ab2 antibody. Likewise, no ATM band was detected in ATR immunoprecipitates probed with the NB 100–104 antibody (Novus Biologicals) (data not shown).

The beads were washed once with immunoprecipitation buffer, once with immunoprecipitation buffer containing 0.5 M LiCl, and three times with kinase buffer (50 mM HEPES, pH 7.5, 50 mM NaCl, 1 mM DTT, 10 mM $MgCl_2$, 10 mM $MnCl_2$, and 50 mM β-glycerophosphate). The beads were then incubated for 30 min at 30°C with 0.5 μg of the substrate PHAS-I (phosphorylated heat- and acid-stable protein regulated by insulin) (Stratagene, Amsterdam-Zuidoost, The Netherlands) in 30 μl of kinase buffer containing 20 μM unlabeled ATP and 10 μCi of [γ-^{32}P]ATP. The reaction products were separated on a 15% SDS-polyacrylamide gel. Gels were dried and exposed to Kodak X-OMAT film (Kodak, Rochester, NY) with intensifying screen at −80°C. The immunocomplexes were also subjected to immunoblotting with anti-ATM (NB 100–104; Novus Biologicals) or anti-ATR (Ab2; Oncogene) rabbit polyclonal antibodies to assure equivalent kinase abundance.

Immunofluorescence. For immunofluorescence microscopy of ATR, 2.5×10^4 cells were collected, washed in PBS, and cytospun onto glass coverslips. Before fixation, the in situ cell fractionation was carried out as described by Mirzoeva and Petrini (2001). The cells were fixed in 4% formaldehyde for 10 min and in methanol at −20°C for 2 min, rehydrated in PBS, and then permeabilized in 0.5% Triton X-100 for 10 min at room temperature. Cells were blocked with 10% normal goat serum (Hyclone Laboratories) in PBS for 1 h, and then incubated with a rabbit polyclonal antibody against ATR (Ab-2; Oncogene) overnight at 4°C. Cells were washed with PBS containing 0.2% Tween-20 and overlaid with fluorescein isothiocyanate-conjugated goat anti-rabbit IgG (ICN-Cappel, Irvine, CA) for 45 min at 37°C. Cells were then washed and counterstained with 0.1 μg/ml 4′,6′-diamidino-2-phenylindole for 2 min and the glass slides were mounted with 50% glycerol. Coverslips were analyzed using a Leica DMRB fluorescence microscope equipped with a CCD camera. The images were processed using the IAS 2000 Delta System software and Photoshop 5.5 (Adobe Systems, Mountain View, CA).

Results

Time-Course Analysis of Cell Growth Inhibition, Cell Cycle Perturbation, and Apoptosis Induced by TMZ in TK6 and MT1 Cells. We have shown previously that proliferation of the lymphoblastoid TK6 cells was markedly impaired by 12.5 μM TMZ, whereas MT1 cells were completely resistant to this drug concentration (D'Atri et al., 1998). To elucidate the early molecular events triggered exclusively by the engagement of the MMR system in cells exposed to O^6-G–methylating agents, we treated both cell lines with this TMZ concentration. To analyze the molecular mechanisms underlying cell growth inhibition induced by high concentrations of O^6-G–methylating agents in MMR-deficient cells, we treated the MT1 cells with 1.2 mM TMZ, because this drug concentration was found to produce a cell growth inhibition comparable with that produced in TK6 cells by 12.5 μM TMZ.

We first analyzed the kinetics of cell growth inhibition in

TK6 and MT1 cells treated with equitoxic TMZ concentrations and, as a control, in MT1 cells exposed to 12.5 μM TMZ. Figure 1A shows that during the first 24 h, drug-treated TK6 cells doubled in number but then stopped growing and their numbers declined after 48 and 72 h of culture. In MT1 cells exposed to 1.2 mM TMZ, cell growth arrest occurred immediately after drug treatment and remained detectable up to 48 h. The cells started to regrow at 72 h (Fig. 1A). No impairment of proliferation was observed in MT1 cells treated with 12.5 μM TMZ (data not shown).

We next performed a time-course analysis of TMZ-induced cell cycle perturbations and apoptosis. As illustrated in Table 1 and Fig. 1B, no cell cycle perturbations were detected in TMZ-treated TK6 cells during the first 18 h. After 24 h, a decrease in the G_1 fraction and a moderate increase in the S and G_2 fractions were observed. The number of cells in middle and late S phase further increased after 30 and 36 h and then returned to values similar to those of untreated cells. The proportion of cells in G_1 further decreased at 30 and 36 h and remained lower than that of controls up to 48 h. The percentage of cells in G_2 remained substantially unchanged from 24 to 36 h and slightly increased at 42 and 48 h. The

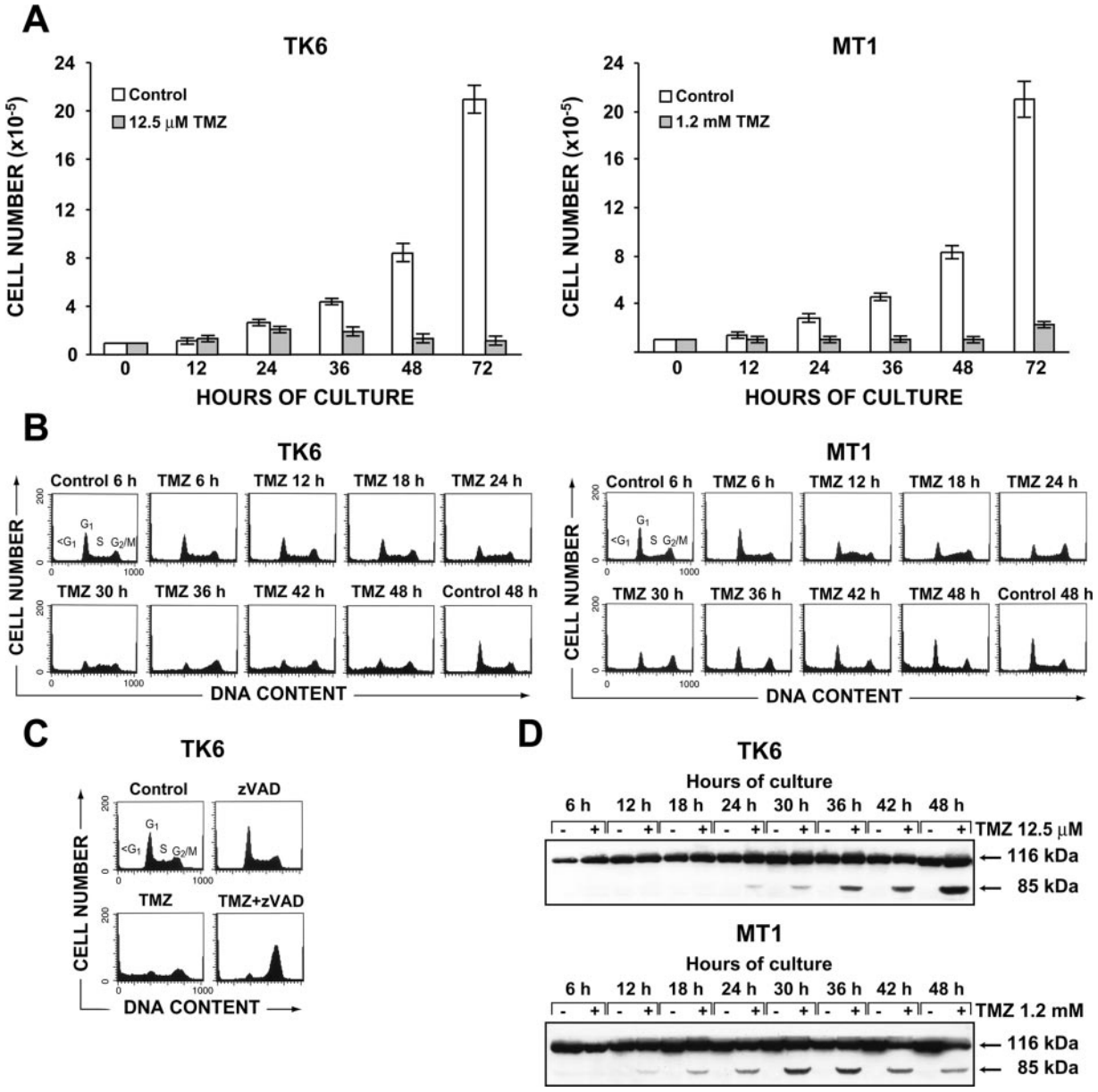

Fig. 1. Kinetics of cell growth inhibition, cell cycle perturbation, and apoptosis induced by equitoxic concentrations of TMZ in TK6 and MT1 cells. A, kinetics of cell growth inhibition. TK6 and MT1 cells were incubated in CM or CM containing TMZ for 72 h. Cell growth was evaluated in terms of viable cell count at the indicated time points. Each value represents the mean of three independent experiments, with bars indicating S.E.M. B, kinetics of cell cycle perturbations and apoptosis. TK6 and MT1 cells were incubated in CM or CM containing 12.5 μM TMZ (TK6 cells) or 1.2 mM TMZ (MT1 cells) for 48 h. At the indicated time points, the cells were harvested and processed for flow cytometric analysis of DNA content. C, effect of the pan-caspase inhibitor zVAD-fmk on cell cycle perturbation and apoptosis induced by TMZ in TK6 cells. The cells were incubated in CM or CM containing either 200 μM zVAD-fmk, 12.5 μM TMZ, or both agents for 48 h and then processed for the analysis of DNA content. D, kinetics of PARP cleavage. TK6 and MT1 cells were cultured in CM or CM containing the indicated concentrations of TMZ for 48 h. Every 6 h, total cell lysates were prepared and analyzed by immunoblotting. Cell extracts were subjected to electrophoresis on an 8% SDS-polyacrylamide gel, transferred to a nitrocellulose membrane, and probed with an anti-PARP mAb. The immune complexes were visualized using ECL.

fraction of cells with hypodiploid DNA content progressively increased from 30 to 48 h. Apoptosis was further confirmed in TMZ-treated TK6 cells by Western blot analysis of PARP cleavage. As illustrated in Fig. 1D, the 85-kDa product of PARP cleavage became faintly detectable after 24 to 30 h of drug exposure and progressively increased up to 48 h. It is noteworthy that when TMZ-induced apoptosis was prevented by the pan-caspase inhibitor zVAD-fmk, the majority of TK6 cells were arrested at the G_2/M phase of the cell cycle after 48 h of culture (Fig. 1C). Taken together, these results indicate that after a transient slowing of the second S phase, TMZ-treated TK6 cells underwent a G_2/M arrest that was followed rapidly by apoptosis. Apoptotic cells coming from the G_2/M phase localized under the S and G_1 cells before reaching a hypodiploid DNA content, leading to an overestimation of the percentage of cells in S and G_1.

As illustrated in Table 1 and Fig. 1B, in MT1 cells treated with 1.2 mM TMZ, a transient increase in the fraction of cells in S phase was detectable from 6 to 18 h, whereas an accumulation of cells in the G_2/M phase was observed from 24 to 36 h. The cells started to recover from the G_2/M arrest after 42 h of culture. An increase in the fraction of cells with hypodiploid DNA content became detectable between 24 and 48 h of culture. PARP cleavage was evident after 12 h, reached a peak between 30 and 36 h, and then began to decrease (Fig. 1D). Thus, also in MT1 cells, PARP cleavage seemed to be an earlier marker of TMZ-induced apoptosis than the appearance of cells with a hypodiploid DNA content. Neither cell cycle perturbations nor apoptosis were detected in MT1 cells exposed to 12.5 μM TMZ (data not shown).

p53 Is Phosphorylated at Multiple Sites in TK6 and MT1 Cells Treated with Equitoxic Concentrations of TMZ, but Not in MT1 Cells Exposed to Low Drug Concentrations. We have previously shown that 12.5 μM TMZ induced p53 stabilization and p21/waf1 up-regulation in the MMR-proficient cell line TK6 but not in its MMR-deficient subline MT1 (D'Atri et al., 1998). To gain further insight into the signaling pathways leading to p53 stabilization and activation in TMZ-treated cells and into the role played by the MMR system in this process, we carried out a time-course analysis of the phosphorylation status of Ser9, Ser15, Ser20, Ser37, Ser46, and Ser392 of p53 in TK6 cells exposed to 12.5 μM TMZ and in MT1 cells treated with either 12.5 μM or 1.2 mM TMZ. Each of the residues analyzed was previously shown to undergo phosphorylation in response to DNA damage (Sionov and Haupt, 1999; Higashimoto et al., 2000; Saito et al., 2002). In both cell lines, we also evaluated the levels of p53 and p21/waf1 proteins. As illustrated in Fig. 2A, we confirmed that TMZ treatment of TK6 cells induced a progressive increase in the amount of p53 and p21/waf1 proteins that was already evident, albeit only at low levels, after 6 h of culture. p53 phosphorylation of Ser15 in TMZ-treated TK6 cells was clearly detected after 6 h, whereas Ser20 and Ser37 seemed phosphorylated only after 12 h. Phosphorylation of Ser9, Ser392, and Ser46 was detectable only after 18 h (Fig. 2A). No p53 phosphorylation was observed in MT1 cells exposed to 12.5 μM TMZ (data not shown), whereas p53 and p21 accumulation and p53 phosphorylation at all the residues under investigation were detected in MT1 cells exposed to 1.2 mM TMZ (Fig. 2B). However, in the latter experiment, phosphorylation of p53 occurred with faster kinetics than in TK6 cells treated with 12.5 μM TMZ, such that most residues were phosphorylated already after 6 h; the exception was Ser9, which seemed phosphorylated only after 12 h. Moreover, in contrast to TK6 cells, the levels of phosphorylated p53 began to decrease after 42 to 48 h of culture.

Because Ser15 was phosphorylated in TMZ-treated TK6 cells after 6 h and, in MT1 cells treated with 1.2 mM TMZ, five of the six p53 sites under investigation were phosphorylated at the same time point, we analyzed the p53 phosphorylation status in both cell lines 1 and 3 h after TMZ exposure. As illustrated in Fig. 2C, in TMZ-treated MT1 cells, phosphorylation of Ser15 was already detectable after 1 h of treatment, whereas phosphorylation of Ser20, Ser37, Ser46, and Ser392, was detectable after 3 h. In TK6 cells, phosphorylation of Ser15 was barely detectable after 3 h of culture (data not shown).

Both Chk1 and Chk2 Kinases Are Phosphorylated in TK6 and MT1 Cells Treated with Equitoxic Concentrations of TMZ but Not in MT1 Cells Treated with Low Drug Concentrations. p53 phosphorylation at Ser20 can be

TABLE 1

Time course analysis of cell cycle perturbations and apoptosis induced by equitoxic concentrations of TMZ in TK6 and MT1 cell lines

The cells were incubated in CM or in CM containing 12.5 μM TMZ (TK6 cells) or 1.2 mM TMZ (MT1 cells) for 48 h. At the indicated time, the cells were processed for analysis of cell cycle perturbation and apoptosis induction. The percentage of cells in each phase of the cell cycle or in apoptosis was evaluated by flow cytometric analysis of DNA content. Data represent the means of four independent experiments, with S.E. not exceeding 10 to 15% of the mean.

Drug	Hours	TK6				MT1			
		Apoptosis	G_1/G_0	S	G_2/M	Apoptosis	G_1/G_0	S	G_2/M
					%				
None	6	10	31	54	15	9	35	53	12
TMZ		12	30	56	14	9	31	63	6
None	12	11	30	60	10	8	36	54	10
TMZ		13	27	58	15	10	20	71	9
None	18	12	28	61	11	8	31	59	10
TMZ		12	24	61	15	12	19	72	9
None	24	11	29	59	12	6	33	56	11
TMZ		14	18	65	17	17	18	66	16
None	30	11	28	59	13	6	32	57	11
TMZ		20	12	72	16	20	22	56	22
None	36	8	28	62	10	4	35	54	11
TMZ		26	10	74	16	24	31	41	28
None	42	8	26	63	11	5	30	59	11
TMZ		34	16	66	18	28	38	42	20
None	48	7	26	62	12	4	32	57	11
TMZ		40	16	64	20	31	38	45	17

mediated by both Chk1 and Chk2 kinases. In vivo activation of Chk1 requires phosphorylation on Ser345 and Ser317 (Zhao and Piwnica-Worms, 2001), whereas activation of Chk2 requires phosphorylation on Thr68 (Bartek et al., 2001). We therefore carried out a time-course analysis of the levels of the two phosphorylated proteins in TK6 cells treated with 12.5 μM TMZ and in MT1 cells exposed to either 12.5 μM or 1.2 mM TMZ. In TMZ-treated TK6 cells, an increase in the level of phosphorylated Chk1 (Ser345) and Chk2 (Thr68) became detectable after 12 h (Fig. 3A). The level of phosphorylated Chk1 was initially higher than that of phosphorylated Chk2, reached a peak at 30 to 36 h, and then began to decrease. The level of phosphorylated Chk2 progressively increased up to 48 h. No changes in the amount of total Chk1 or Chk2 were observed (Fig. 3A). Phosphorylation of Chk1 and Chk2 did not occur in MT1 cells treated with 12.5 μM TMZ (data not shown), but both kinases were phosphorylated in the cells exposed to high drug concentration (Fig. 3B). In this case, the increase in the levels of phosphorylated Chk1 and Chk2 was already detectable after 1 h (Fig. 3C). The level of phosphorylated Chk1 remained elevated up to 18–24 h and then began to decrease, whereas the amount of phosphorylated Chk2 remained elevated up to 48 h. As in the case of TK6 cells, no changes were found in the levels of total Chk1 and Chk2 (Fig. 3, B and C).

ATM and ATR Are Activated in TK6 and MT1 Cells Treated with Equitoxic Concentrations of TMZ but Not in MT1 Cells Treated with Low Drug Concentrations. The Chk1 and Chk2 kinases are downstream targets

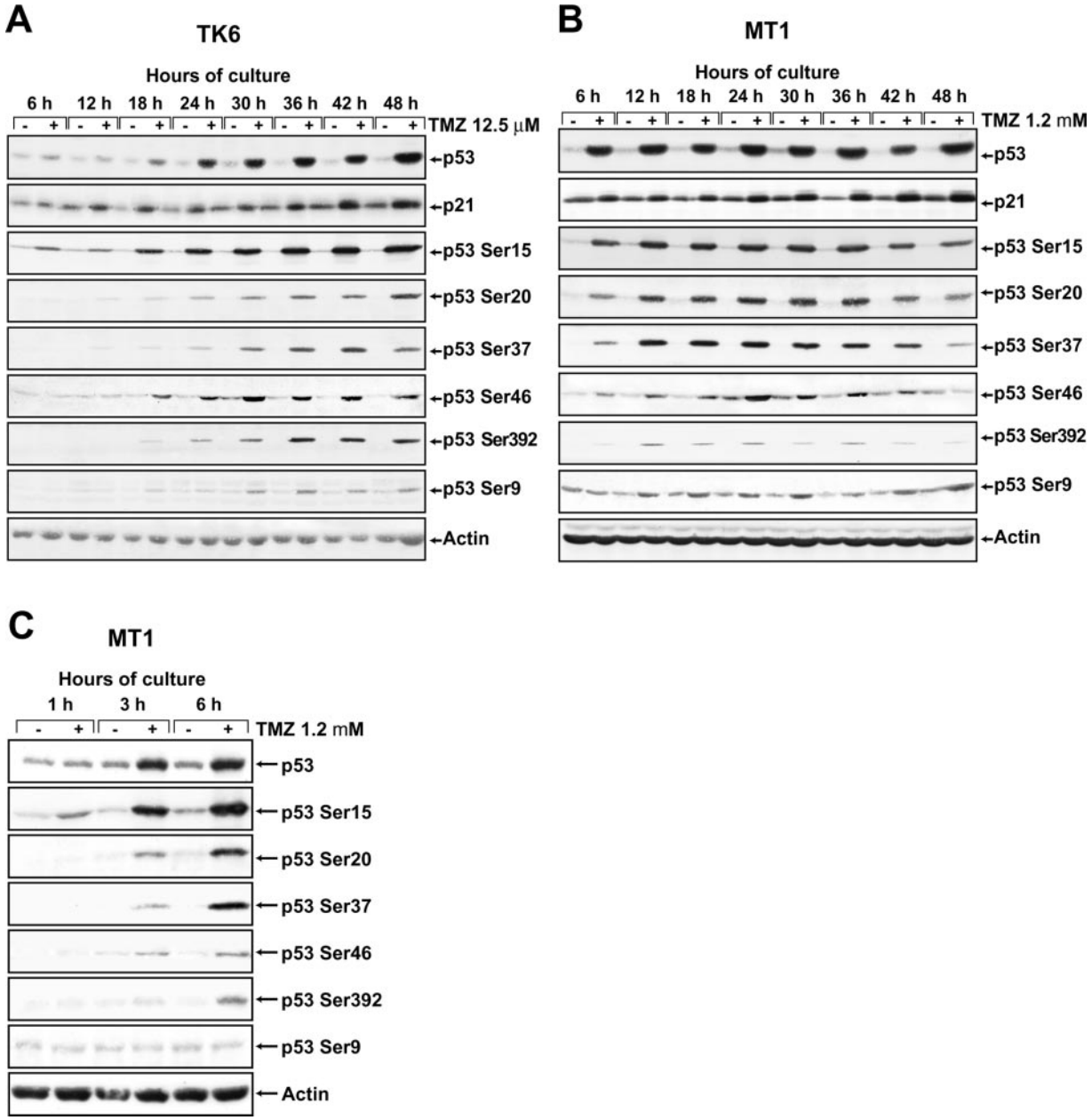

Fig. 2. Kinetics of p53 and p21/waf1 accumulation and of p53 phosphorylation induced by equitoxic concentrations of TMZ in TK6 and MT1 cells. TK6 (A) and MT1 cells (B and C) were cultured in CM or CM containing TMZ, and total cell extracts were prepared at the indicated time points. Cell extracts were subjected to electrophoresis on a 10% (p53 and phosphorylated p53) or 12% (p21/waf1) SDS-polyacrylamide gels, transferred to nitrocellulose membranes, and probed with antibodies against p53, p21/waf1, or p53 phosphorylated at the indicated residues. Incubation with the anti-actin mAb was performed as a loading control. The immune complexes were visualized using ECL.

of ATM and ATR. Moreover, the two latter kinases are able to phosphorylate p53 on Ser15 and Ser37 and, in cells exposed to IR, ATM is required for phosphorylation of p53 on Ser9 and Ser46 (Saito et al., 2002). We therefore investigated whether ATM and ATR were activated in TK6 and MT1 cells treated with equitoxic concentrations of TMZ and, as a control, in MT1 cells exposed to 12.5 μM TMZ. Neither ATM nor ATR was activated in MT1 cells treated with 12.5 μM TMZ (data not shown). As illustrated in Fig. 4A, the kinase activity of ATM in TK6 cells exposed to TMZ increased after 30 h, reached a peak after 42 h, and then began to decrease. In contrast, the ATR kinase activity was already markedly increased after 6 h of culture and remained elevated up to 42 h. A moderate increase in ATR activity was also observed even after 1 and 3 h (data not shown). In MT1 cells exposed to 1.2 mM TMZ, the kinase activities of both ATM and ATR were increased after 6 h. ATM activity reached a peak after 24 h and returned to control levels at 36 h, whereas ATR activity remained elevated up to 42 h (Fig. 4B). In TMZ-treated MT1 cells, the kinase activities of ATM and ATR were also higher than control after 1 and 3 h (data not shown). When cell extracts obtained from untreated or TMZ-treated TK6 and MT1 cells were tested with rabbit IgG instead of anti-ATM or anti-ATR antibodies, incubation of the immunoprecipitate with PHAS-I gave rise to no detectable phosphorylation (data not shown). This finding eliminates the possibility that a nonspecific kinase was responsible for the observed PHAS-I phosphorylation detected in the specific ATM and ATR immunoprecipitates.

To further confirm activation of ATR in TK6 and MT1 cells treated with equitoxic concentrations of TMZ, we examined whether ATR formed characteristic nuclear foci in response to drug treatment in these cells. TK6 and MT1 cells were incubated in the presence of 12.5 μM or 1.2 mM TMZ, respectively, and were stained for ATR after 1, 6, 12, 24, and 42 h. Untreated TK6 and MT1 cells showed a diffuse nuclear staining pattern, but TMZ-treated cells showed distinct nuclear foci at all time points (Fig. 4C and data not shown).

ATM-Deficient Cells Are More Sensitive to TMZ than ATM-Proficient Cells, but Do Not Show an Impairment of p53, Chk1, and Chk2 Phosphorylation after Treatment with Low Concentrations of the Drug. The finding that activation of ATM in TK6 cells exposed to 12.5 μM TMZ occurred only after 30 h of culture indicated that this kinase was not involved in the early phosphorylation of p53, Chk1, and Chk2 induced by low concentrations of the drug. However, we could not exclude the possibility that ATM contributed to the phosphorylation of the three proteins at later times after drug treatment or that it affected cellular responses to TMZ through phosphorylation of other downstream targets. We therefore evaluated the effect of ATM deficiency on growth inhibition, cell cycle perturbation, and apoptosis, as well as on phosphorylation of p53, Chk1, and Chk2 brought about by low TMZ concentrations. To this end, we used the ATM-deficient cell line KT, stably transfected with either a $CdCl_2$-inducible ATM cDNA expression vector (KT MAT1 cells) or with the empty vector only (KT MEP cells).

To verify that the ATM protein expressed in the KT MAT1 cells (Fig. 5A) was functional, we exposed both KT MAT1 and KT MEP cells to IR (10 Gy) and examined the p53 accumulation and Ser15 phosphorylation at selected time intervals up to 24 h after treatment. The KT MAT1 cells responded rapidly to IR with stabilization and phosphorylation of p53. In contrast, accumulation of p53 in KT MEP cells was re-

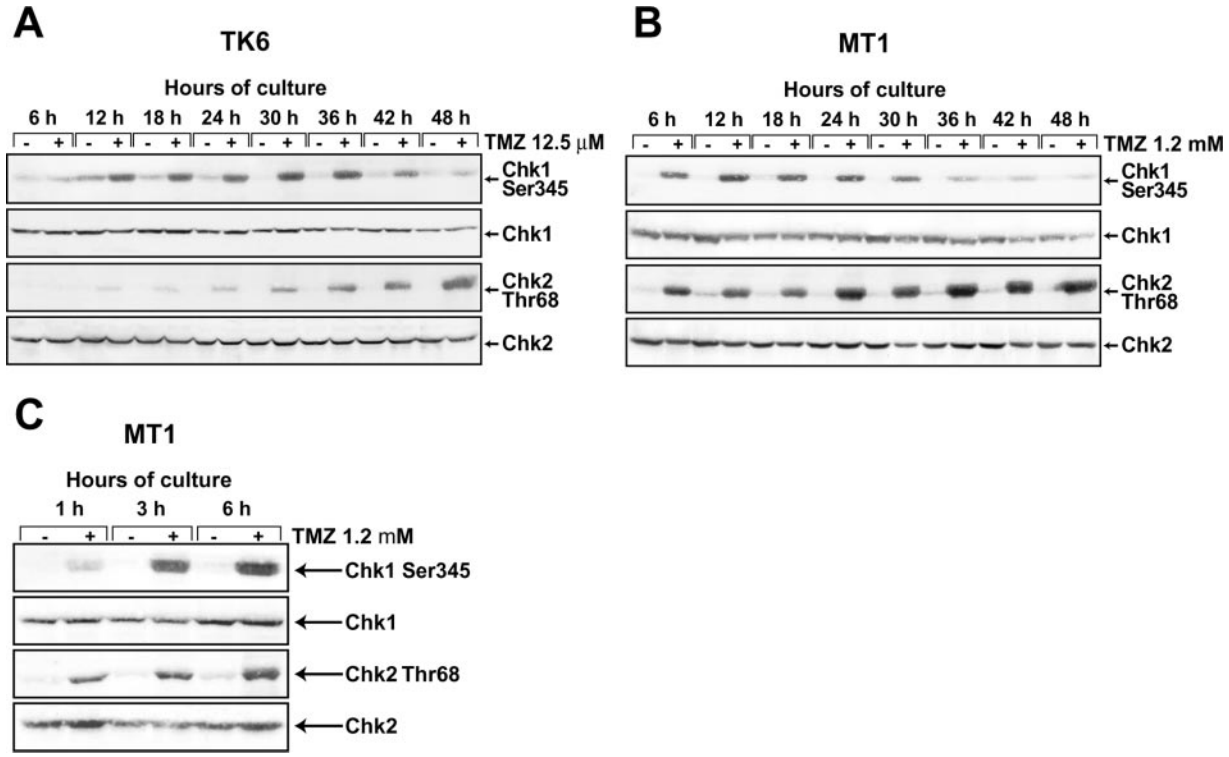

Fig. 3. Kinetics of Chk1 and Chk2 phosphorylation induced by equitoxic concentrations of TMZ in TK6 and MT1 cells. TK6 (A) and MT1 cells (B and C) were cultured in CM or CM containing TMZ, and total cell extracts were prepared at the indicated time points. Cell extracts were subjected to electrophoresis on a 10% SDS-polyacrylamide gel, transferred to a nitrocellulose membrane, and probed with antibodies against Chk1, Chk2, phospho-Chk1 (Ser345), and phospho-Chk2 (Thr68). The immune complexes were visualized using ECL.

tarded and its phosphorylation on Ser15 was impaired up to 1 h after irradiation (Fig. 5B).

We then tested the susceptibility of these lines to TMZ-induced growth inhibition. All the experiments were performed in the presence of 10 μM BG to inhibit the repair of O^6-MeG. The results illustrated in Fig. 6A show that the ATM-deficient cell line was significantly more sensitive to TMZ than its ATM-proficient counterpart.

A time-course analysis of cell cycle perturbation and induction of apoptosis in KT MAT1 and KT MEP cells exposed to 10 μM TMZ (plus BG) was then carried out. The proportions of cells with hypodiploid DNA content or in the different phases of the cell cycle are reported in Table 2 and Fig. 6B. No cell cycle alterations were observed in TMZ-treated KT MAT1 and KT MEP cells during the first 18 h of culture, whereas at 24 h, a decrease in the fraction of cells in the G_1 phase accompanied by a corresponding increase in the number of cells in the S phase became detectable in both cell lines. From 30 to 48 h, both cell types began to accumulate in the G_2/M phase; this accumulation was more apparent in KT MEP cells and was accompanied by a corresponding decrease in the number of cells in G_1. The fraction of cells in S, still slightly higher than in controls after 30 h, progressively decreased from 36 to 48 h. After 72 h, drug-treated KT MAT1 and KT MEP cells started to recover from the G_2 block, as indicated by the increase in the number of cells in G_1 and the decrease in the fraction of cells in G_2/M. However, in the KT MEP cell line, the recovery was less pronounced than in KT MAT1 cells. No significant differences in the fractions of apoptotic cells were found between the two cell lines upon exposure to TMZ.

Finally, we evaluated p53 accumulation and phosphorylation of Chk1, Chk2, and p53 on Ser15 in both cell lines upon TMZ treatment. The cells were cultured in the presence of 10 μM TMZ (plus BG) for 72 h and analyzed every 24 h. In both drug-treated cell lines, p53 accumulation and phosphorylation of Chk1, Chk2, and p53 on Ser15 were comparable at all time points (data not shown).

ATM-Deficient Cells Show Impaired Phosphorylation of Chk1, Chk2, and p53 at Early Time Points after Treatment with High Concentrations of TMZ. The re-

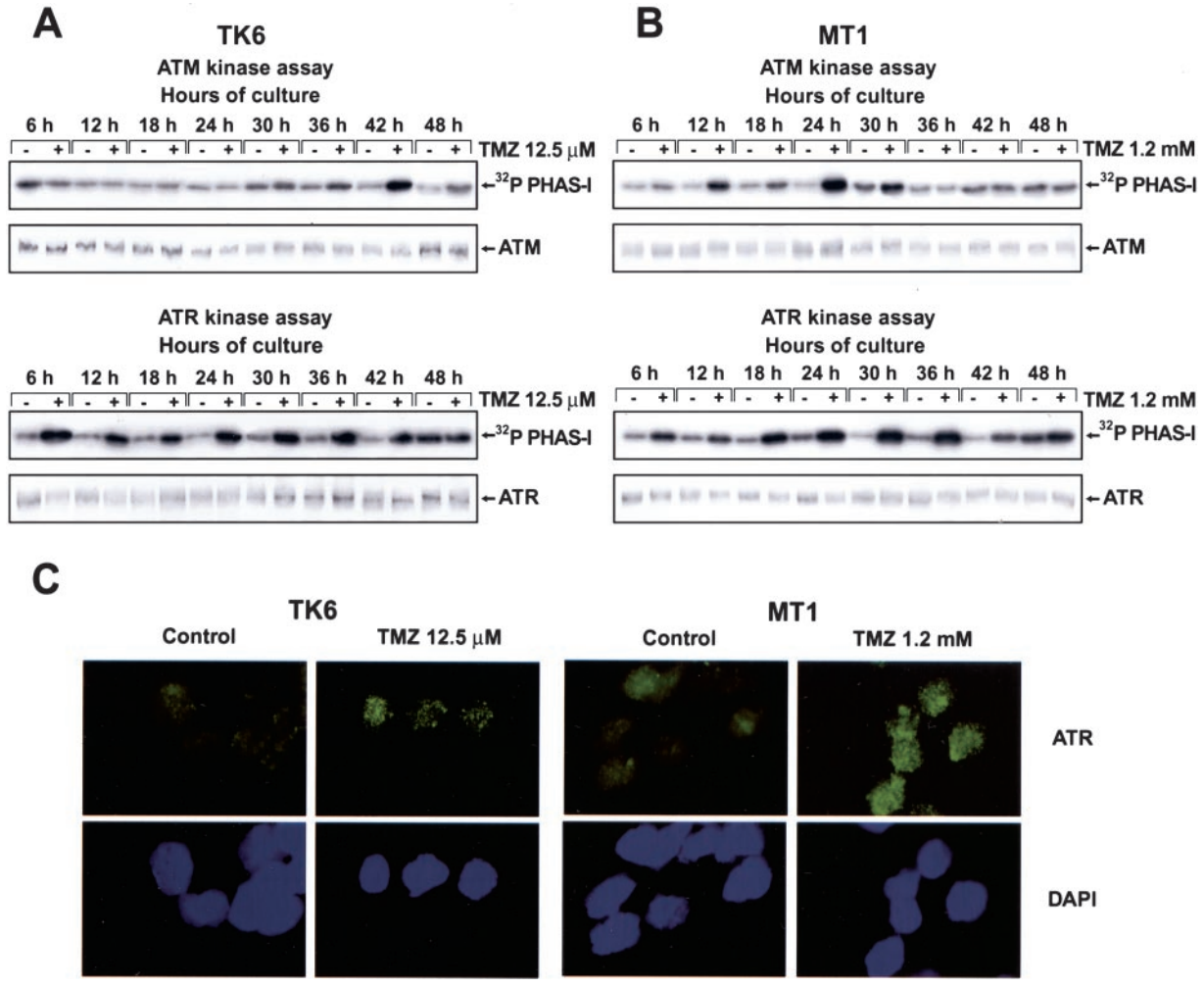

Fig. 4. Kinetics of ATM and ATR activation in TK6 and MT1 cells treated with equitoxic concentrations of TMZ. TK6 (A) and MT1 (B) cells were cultured in CM or CM containing TMZ for 48 h. At the indicated time points, ATM or ATR was immunoprecipitated, and kinase activity was assayed using PHAS-I as substrate. The reaction products were run on a 15% SDS-polyacrylamide gel and visualized by autoradiography. Immunoprecipitates were also immunoblotted with anti-ATM or anti-ATR antibodies to assure equivalent kinase abundance. C, alterations in ATR subcellular localization induced by equitoxic concentrations of TMZ in TK6 and MT1 cells. TK6 and MT1 cells were incubated in CM or CM containing TMZ for 24 or 1 h, respectively. The cells were then harvested, washed, cytospun onto glass coverslips, and processed for immunostaining with the anti-ATR antibody Ab-2 as described under *Materials and Methods*. The percentage of foci-positive cells was 20% in TMZ-treated TK6 cells and 25% in TMZ-treated MT1 cells. Similar results were obtained in two additional independent experiments.

sults obtained with MT1 cells exposed to 1.2 mM TMZ indicated that, in response to high TMZ concentrations, both ATM and ATR were rapidly activated also in the absence of a functional MMR system.

To evaluate the contribution of ATM to phosphorylation of Chk1, Chk2, and p53 on Ser15 induced by high TMZ concentrations, KT MAT1 and KT MEP cells were cultured in the presence of 1.2 mM TMZ (plus 10 μM BG) and analyzed for these molecular events after 1, 3, 6, 12, and 24 h of drug exposure.

The results illustrated in Fig. 7 show that the kinetics of Chk1, Chk2, and p53 phosphorylation in TMZ-treated KT MAT1 cells was comparable with that observed previously in MT1 cells exposed to the same drug concentration. After 1 and 3 h of culture in the presence of the drug, p53 and Chk1 phosphorylation was moderately reduced in KT MEP cells with respect to KT MAT1, whereas no differences between the two cell lines existed at later time points (Fig. 7). TMZ-induced phosphorylation of Chk2 was markedly impaired in KT MEP cells up to 6 h of culture but became comparable with that observed in TMZ-treated KT MAT1 cells at later time points (Fig. 7).

ATR Is Required for Efficient Phosphorylation of Chk1 and p53 on Ser15 in Response to TMZ. To investigate the role of ATR in the phosphorylation of p53, Chk1, and Chk2 in cells exposed to low or high TMZ concentrations, we used the U2OS cells stably-transfected with a doxycycline-inducible ATR-kd expression construct. This cell line had undetectable expression of the FLAG-tagged ATR-kd in the absence of doxycycline. Doxycycline induction resulted in greatly increased levels of ATR-kd as monitored by Western blotting (Fig. 8).

In a first set of experiments, uninduced or ATR-kd–overexpressing U2OS cells were incubated with 25 μM TMZ plus 10 μM BG and analyzed for phosphorylation of Chk1, Chk2, and p53 on Ser15 after 12, 24, and 48 h of culture. In a second set of experiments, the cells were incubated with 1.2 mM TMZ (plus BG) and analyzed for the same parameters after 1, 3, 6, 12, and 24 h.

The results illustrated in Fig. 8A show that after 12 and 24 h of culture in the presence of 25 μM TMZ, p53 phosphorylation was moderately reduced in the ATR-kd–overexpressing cells compared with uninduced cells, whereas after 48 h of culture, p53 phosphorylation was comparable in both uninduced and induced cells. Chk1 phosphorylation triggered by TMZ was strongly impaired in ATR-kd–overexpressing cells at all the time points analyzed, whereas Chk2 phosphorylation remained essentially unchanged.

Upon treatment with 1.2 mM TMZ, p53, Chk1, and Chk2 were rapidly phosphorylated in uninduced cells (Fig. 8B). In ATR-kd–overexpressing cells, TMZ-induced Chk1 phosphorylation was markedly impaired at all the time points analyzed, whereas phosphorylation of p53 and Chk2 was unaffected (Fig. 8B).

ATR-kd Overexpressing Cells Show an Impairment of G_2/M Arrest Triggered by Low TMZ Concentrations and Are More Susceptible to Cell Growth Inhibition Induced by the Drug. To better define the linkage between ATR activation and G_2/M arrest triggered by low TMZ concentrations, uninduced and ATR-kd-overexpressing U2OS cells were incubated with 25 μM TMZ (plus BG) and analyzed for cell cycle perturbations after 48 h of culture. The results of a representative experiment illustrated in Fig. 9 show that G_2/M arrest triggered by TMZ treatment was substantially attenuated in ATR-kd–overexpressing cells compared with uninduced cells.

We also evaluated the effect of ATR ablation on cell sensitivity to low TMZ concentrations. To this end, uninduced and ATR-kd–overexpressing cells were incubated with 25 μM TMZ (plus BG) and analyzed for cell growth after 96 h of culture. Under these experimental conditions, the percentage of cell growth of TMZ-treated groups with respect to untreated controls was 26 $\pm$ 1.2 in the case of uninduced cells and 14 $\pm$ 0.6 in the case of ATR-kd–overexpressing cells; each value represented the mean $\pm$ standard error of three independent experiments.

Discussion

In this study, we demonstrate that activation of ATM and ATR and phosphorylation of Chk1, Chk2, and p53 occur in response to TMZ and that these molecular events are abso-

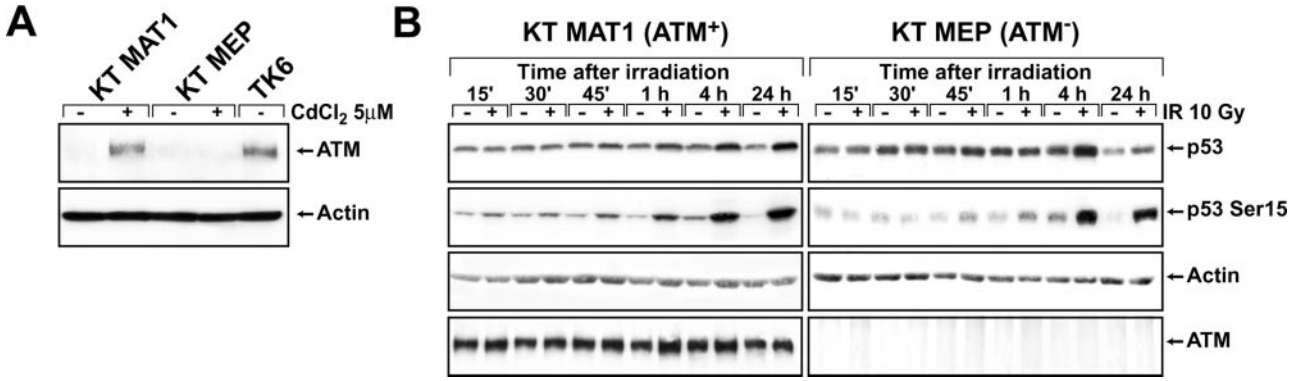

Fig. 5. Functional characterization of KT MAT1 and KT MEP cell lines. A, total cell lysates were prepared from KT MAT1 and KT MEP cells exposed for 16 h to 5 μM $CdCl_2$. Cell extracts were subjected to electrophoresis on a 6% SDS-polyacrylamide gel, transferred to nitrocellulose membranes, and probed with the anti-ATM antibody NB 100–104. Incubation with the anti-actin mAb was performed as a loading control. The immune complexes were visualized using ECL. B, KT MAT1 and KT MEP cells were treated with 5 μM $CdCl_2$ for 16 h, washed, suspended in CM, exposed to 10 Gy of IR, and analyzed for p53 accumulation and phosphorylation on Ser15 at the indicated time points. Total cell extracts were resolved on 10% SDS polyacrylamide gels, transferred to nitrocellulose membranes, and probed with polyclonal antibodies against p53 and phospho-p53 (Ser15). Incubation with the anti-actin mAb was performed as a loading control. For ATM detection, cell lysates were resolved on 6% SDS polyacrylamide gels, and the membranes were probed with the anti-ATM antibody NB 100–104. The immune complexes were visualized using ECL.

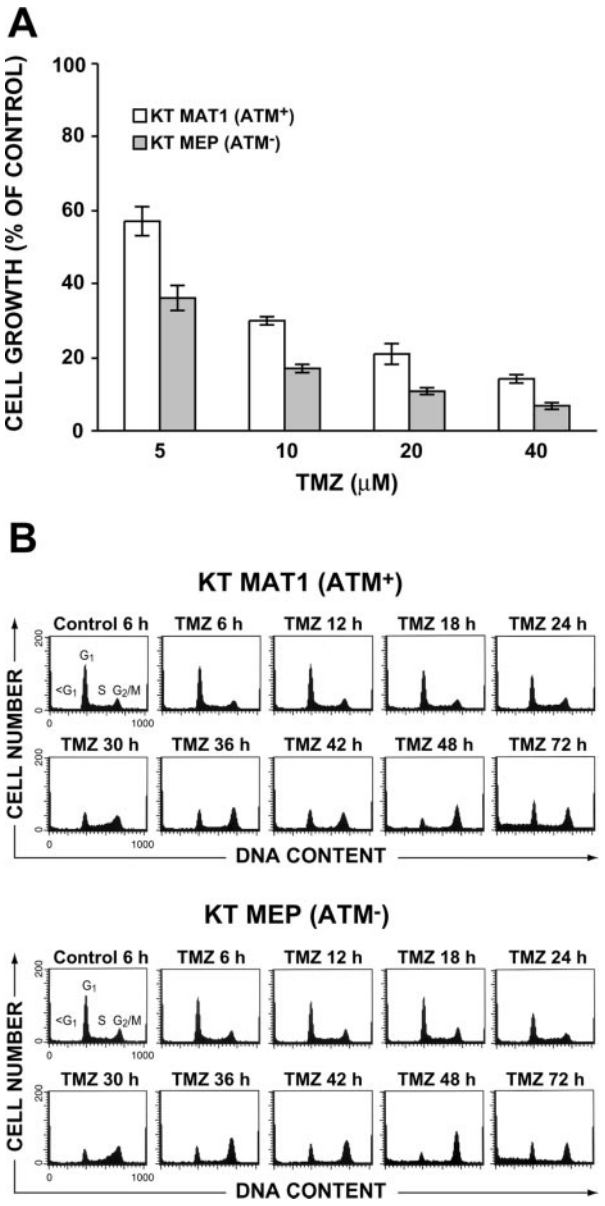

Fig. 6. Cell growth inhibition, cycle perturbations, and apoptosis induced by low TMZ concentrations in KT MAT1 and KT MEP cells. A, cell growth inhibition. The cells were exposed to $CdCl_2$, BG, and TMZ as described under *Materials and Methods*, and cell growth was evaluated after 72 h of culture in terms of viable cell count. Data are expressed in terms of percentage of cell growth of drug-treated groups with respect to controls. Each value represents the mean of three independent experiments, with bars indicating S.E.M. The number of cells per milliliter in the untreated cultures at the end of the assay was $9.5 \pm 0.75 \times 10^5$ for KT MAT1 cells and $9.9 \pm 0.43 \times 10^5$ for KT MEP cells. For each experiment, the TMZ IC_{50} value (i.e., the drug concentration producing 50% inhibition of cell growth, calculated on the regression line in which cell number was plotted against the logarithm of drug concentration) for KT MAT1 and KT MEP cells was also determined. The mean TMZ IC_{50} values ± S.E. were 5.45 ± 0.78 μM for KT MAT1 cells and 1.48 ± 0.36 μM for KT MEP cells. The difference was statistically significant according to Student's t test ($p < 0.01$). B, kinetics of cell cycle perturbations and apoptosis. KT MAT1 and KT MEP treated as in A were collected at the indicated time points and processed for flow cytometric analysis of DNA content.

lutely dependent on a functional MMR system only in cells exposed to low drug concentrations.

Upon treatment with 12.5 μM TMZ, the MMR-proficient TK6 cells transiently slowed in the S-phase and then arrested in the G_2/M phase of the cell cycle, from which they proceeded to apoptosis. All these events occurred in the second cell cycle after treatment and were preceded by activation of ATR, phosphorylation of Chk1 and Chk2, and p53 stabilization and phosphorylation at multiple sites. ATM was also activated in TMZ-treated TK6 cells but only at late time points after drug exposure. Similar treatment of the MMR-deficient MT1 cells failed to induce G_2/M arrest and apoptosis or to activate ATM and ATR and cause phosphorylation of Chk1, Chk2, and p53.

Taken together, these data support the hypothesis that in cells treated with low TMZ concentrations, lesions generated by the unsuccessful processing of O^6-MeG:T mismatches, possibly gaps in the newly synthesized DNA, signal in the first S-phase to ATR. However, the initial activation of ATR was insufficient to bring about cell cycle arrest, and the cells transit through G_2, M, and G_1 and enter the second S-phase, where the single-stranded regions are converted into DSBs during replication (Kaina et al., 1997). These lesions signal to ATM and, directly or indirectly through their processing, sustain ATR activation. The cells, after a transient delay in the S-phase, arrest at the G_2/M phase and initiate apoptosis. In this scenario, ATR seems to be the major kinase responsible for triggering the cell cycle checkpoint, in that its activation in TMZ-treated TK6 cells preceded phosphorylation of p53, Chk1, and Chk2, whereas ATM was activated later. Moreover, after treatment with 10 μM TMZ, neither a defective phosphorylation of Chk1, Chk2, and p53 (on Ser15) nor an impairment of the G_2/M arrest was observed in the ATM-deficient lymphoblastoid cell line KT MEP compared with the ATM-expressing syngenic KT MAT1 cell line.

Our finding that, in cells exposed to low TMZ concentrations, ATM activation is a late event, requires a functional MMR system, and is dispensable for phosphorylation of Chk1, Chk2, and p53 on Ser15 seems to contrast with a recent study by Adamson et al. (2002), which showed that the kinase was rapidly activated in response to MNNG in a MMR-independent fashion and was required for the early phosphorylation of p53 on Ser15. However, as the concentration of MNNG used in the study of Adamson et al. was very high, ATM activation observed by the authors was probably linked to DNA damage distinct from methylation of O^6-G and was, therefore, independent of MMR. Indeed, in MT1 cells treated with 1.2 mM TMZ, we also detected a rapid activation of ATM. Moreover, the kinase seemed to be involved in the early phosphorylation of p53 on Ser15 in cells exposed to high TMZ concentrations.

The involvement of ATR in cell cycle checkpoint activation in response to low TMZ concentrations is further confirmed by the results obtained in U2OS cells induced to overexpress a kinase-dead ATR variant. Upon treatment with 25 μM TMZ, these cells displayed reduced phosphorylation of Chk1 and p53 on Ser15 with respect to uninduced cells. Moreover, they showed an impairment of TMZ-induced G_2/M arrest and were also more susceptible to cell growth inhibition brought about by the drug than uninduced cells, thus indicating that ATR-dependent triggering of the G_2/M arrest protects against TMZ-induced cytotoxicity.

A recent study by Wang and Qin (2003), showed that in MMR-proficient cells exposed to MNNG, ATR was required for Chk1 and SMC1 phosphorylation and for activation of the *S*-phase checkpoint, whereas ATM was dispensable. Our results are consistent with these findings and provide further

insight into the signaling pathways activated in MMR-proficient cells by low concentrations of O^6-G methylating agents. Indeed, we show that both ATR and ATM were functionally activated in response to TMZ, and that the former kinase was involved in the G_2/M arrest induced by the drug. Moreover, we demonstrate that, although dispensable for cell cycle checkpoint activation, ATM conferred protection against TMZ induced cytotoxicity. Indeed, KT MEP cells were about three-fold more sensitive to TMZ than KT MAT1 cells. Compared with KT MAT1, KT MEP cells showed a more pronounced arrest in the G_2/M phase of the cell cycle in response to TMZ treatment, whereas no significant differences in the levels of apoptosis induced by the drug were observed between the two cell lines. This suggests that the increased sensitivity of KT MEP cells to TMZ may be dependent on their reduced ability of recover from the G_2/M block, possibly as a consequence of a reduced ability to repair DSBs arising during the second S-phase after treatment. Indeed, ATM-deficient cells show defects in double-strand break repair after IR (Khanna et al., 2001; Shiloh, 2003).

Recently Hirose et al. (2003) showed that in MMR-proficient glioma cells exposed to TMZ, the mitogen-activated protein kinase p38α was activated in addition to Chk1 and Chk2 and that inhibition of p38α activity was associated with a marked impairment of TMZ-induced G_2/M arrest. Our data on ATR-kd–overexpressing cells treated with 25 μM TMZ strongly suggest that ATR-dependent phosphorylation of Chk1 may have a role in the G_2/M arrest induced by the drug. However, it cannot be excluded that ATR is also required for p38α activation in response to TMZ and that the attenuation of drug-induced G_2/M arrest observed in ATR-kd overexpressing cells also results from a reduced activation of p38α. Further studies will be required to better evaluate the contribution of Chk1, Chk2, and p38α activation to TMZ-induced

TABLE 2

Time-course analysis of cell cycle perturbations and apoptosis induced by TMZ in KT MAT1 and KT MEP cell lines

The cells, after a 16-h exposure to 5 μM $CdCl_2$, were incubated in CM containing 10 μM BG or 10 μM TMZ plus 10 μM BG for 72 h. At the indicated times, the cells were processed for analysis of cell cycle perturbation and apoptosis induction. The percentage of cells in each phase of the cell cycle or in apoptosis was evaluated by flow cytometric analysis of DNA content. Data represent the means of three independent experiments, with S.E. not exceeding 10 to 15% of the mean.

Drug	Hours	KT MAT1				KT MEP			
		Apoptosis	G_1/G_0	S	G_2/M	Apoptosis	G_1/G_0	S	G_2/M
		%							
BG	6	13	43	46	11	15	40	48	12
TMZ/BG		14	44	46	10	13	37	50	13
BG	12	14	45	44	11	12	37	50	13
TMZ/BG		15	43	45	12	11	35	49	16
BG	18	16	44	46	10	13	40	46	14
TMZ/BG		14	42	47	11	13	38	46	16
BG	24	13	45	42	13	11	41	47	12
TMZ/BG		14	35	50	15	14	32	53	15
BG	30	10	45	43	12	9	41	46	13
TMZ/BG		13	28	55	17	14	21	53	26
BG	36	11	44	44	12	10	43	45	12
TMZ/BG		16	18	47	35	16	13	42	45
BG	42	11	46	43	11	9	43	44	13
TMZ/BG		19	22	33	45	15	16	31	53
BG	48	11	44	43	13	10	45	42	13
TMZ/BG		25	21	27	52	23	14	23	63
BG	72	7	47	42	11	5	46	43	11
TMZ/BG		31	37	29	34	29	28	27	45

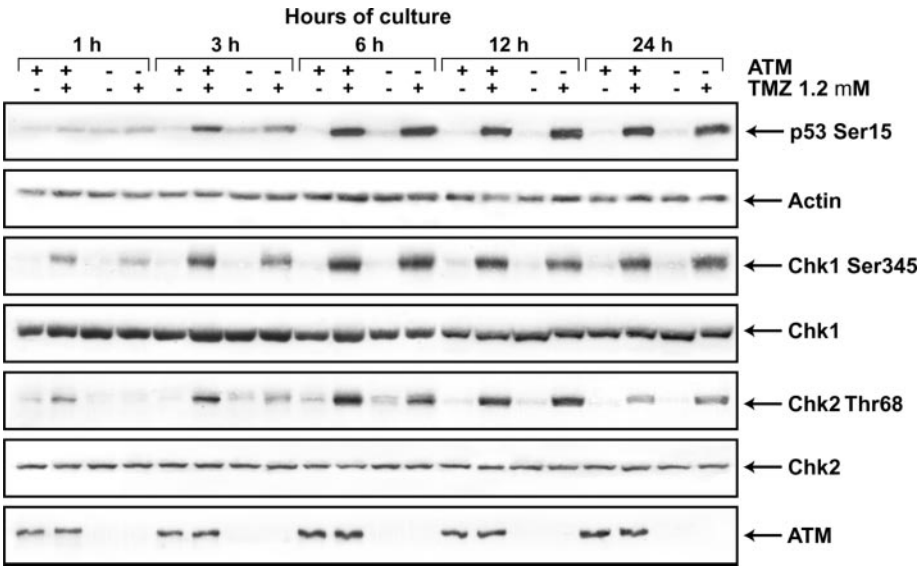

Fig. 7. Effects of ATM deficiency on phosphorylation of Chk1, Chk2, and p53 Ser15 induced by high TMZ concentrations. KT MAT1 and KT MEP cells were exposed to $CdCl_2$, BG (10 μM), and TMZ (1.2 mM), as described under *Materials and Methods*. At the indicated time points, total cell lysates were prepared and analyzed by immunoblotting. Cell extracts were resolved on SDS polyacrylamide gels, transferred to nitrocellulose membranes, and probed with antibodies against phospho-p53 (Ser15), phospho-Chk1 (Ser345), phospho-Chk2 (Thr68), Chk1, Chk2, and ATM. Incubation with the anti-actin mAb was performed as a loading control. The immune complexes were visualized using ECL.

G_2/M arrest and to define whether the Chk1/Chk2 and p38α pathways of G_2/M arrest act independently from each other or whether they are interconnected.

Although a functional MMR system is absolutely required for cell cycle checkpoint activation in cells exposed to low TMZ concentrations, it seems dispensable in cells treated with high concentrations of the drug. Indeed, upon exposure to 1.2 mM TMZ, the MMR-deficient MT1 cell line underwent G_2/M arrest and apoptosis and displayed activation of ATM and ATR, phosphorylation of Chk1 and Chk2, and p53 stabilization, and phosphorylation at multiple sites. Notably, G_2/M arrest and apoptosis in these cells occurred in the first cell cycle after drug treatment, and the kinetics of ATM and ATR activation, as well as those of Chk1, Chk2, and p53 phosphorylation, were faster then those observed in MMR-proficient cells exposed to low TMZ concentrations. On the other hand, no differences in the kinetics of phosphorylation of Chk1, Chk2, and p53 on Ser15 were observed between MMR-proficient and MMR-deficient cells exposed to 1.2 mM TMZ. These findings support the hypothesis that DNA damage leading to activation of ATM- and ATR-dependent signaling pathways is generated by different mechanisms in cells exposed to low or high TMZ concentrations.

In addition to O^6-MeG, TMZ causes base methylation at numerous nucleophilic centers within the DNA, such as the N^7 position of guanine and the N^3 position of adenine. Repair of the latter type of methylation damage is addressed primarily by base excision repair, whereby the modified bases are removed by specialized DNA glycosylases. In the next step of the repair process, the endonuclease HAP-1 creates transient strand breaks by cleaving the sugar/phosphate backbone 5′-from the abasic sites. It is possible that high concentrations of TMZ generate so much base modification that the processing of closely-situated abasic sites on opposite strands of the duplex might result in the generation of DSBs, which would trigger ATM and ATR activation independently of the MMR status of the cells.

In cells exposed to high TMZ concentrations, ATM seems to be required for an efficient phosphorylation of Chk1, Chk2, and p53 on Ser15 at early time points (1–6 h) after treatment. On the other hand, ATR seems necessary for an efficient phosphorylation of Chk1, but not of Chk2 and p53, at

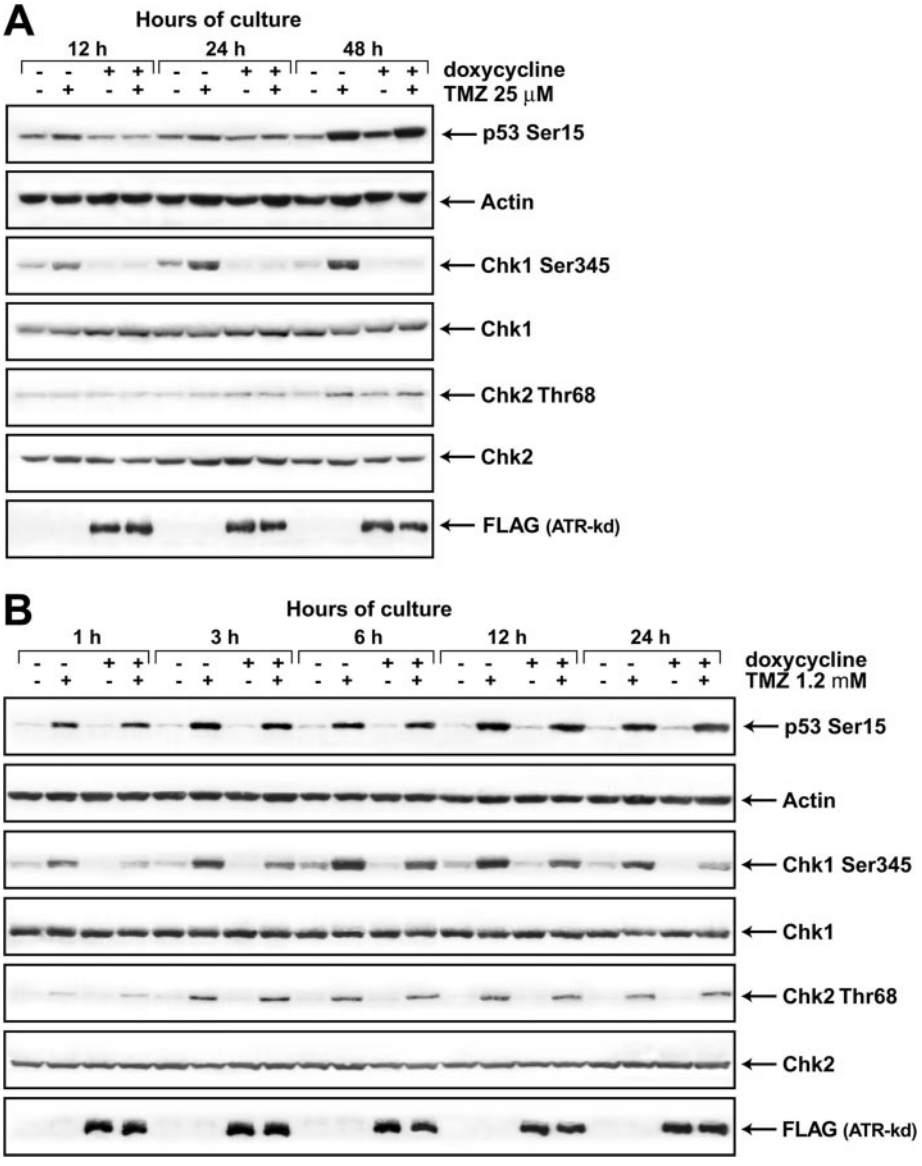

Fig. 8. Effects of ATR inhibition on TMZ-induced phosphorylation of Chk1, Chk2, and p53 Ser15. U2OS cells stably transfected with a doxycycline-inducible ATR-kd expression construct were cultured in the absence or in the presence of 1 μg/ml doxycycline for 24 h. BG (10 μM) and TMZ [either 25 μM (A) or 1.2 mM (B)] were then added to the cultures as described under *Materials and Methods*. Control groups were treated only with BG or doxycycline plus BG. At the indicated time points, the cells were recovered, and whole-cell lysates were prepared. Cell extracts were resolved on SDS polyacrylamide gels, transferred to nitrocellulose membranes, and probed with antibodies against phospho-p53 (Ser15), phospho-Chk1 (Ser345), phospho-Chk2 (Thr68), Chk1, Chk2, and FLAG sequence. Incubation with the anti-actin mAb was performed as a loading control. The immune complexes were visualized using ECL.

least up to 24 h after treatment. A large body of experimental evidence indicates that Chk1 is essential for the G_2 checkpoint induced by various DNA-damaging agents (Liu et al., 2000; Rhind and Russell, 2000; Zhou and Elledge, 2000; Abraham, 2001). In contrast, the role of Chk2 in DNA-damage induced G_2 checkpoint is still controversial. For instance, Chk2-null mutant embryonic stem cells have been shown to be defective in maintaining but not initiating G_2 arrest in response to IR (Hirao et al., 2000). However, recent studies using Chk2 knockout mice have shown that both the initiation and maintenance of the IR-induced G_2 checkpoint are normal in Chk2-deficient embryonic stem cells (Takai et al., 2002). It is thus tempting to speculate that at early time points after treatment with high TMZ concentrations, both ATM and ATR contribute to G_2/M arrest through phosphorylation of Chk1, whereas ATR plays a major role in the late phase of the response. Studies aiming to verify this hypothesis are currently in progress.

Beside ATR, ATM, Chk1, and Chk2, other cellular kinases are likely to be activated in response to TMZ and, through phosphorylation of specific targets, play a role in cell cycle arrest, apoptosis or repair of DNA damage. The results of our study provide preliminary indications about the kinases possibly involved in p53 stabilization and functional activation. In TK6 and MT1 cells treated with equitoxic concentrations of TMZ, p53 was phosphorylated on Ser9, Ser15, Ser20, Ser37, Ser46, and Ser392. Although Ser15, Ser20, and Ser37 are direct targets of either ATR/ATM (Ser15 and Ser37) or Chk1/Chk2 (Ser20), Ser9, Ser46, and Ser392 are not phosphorylated by these kinases. Previous studies have shown that casein kinase I phosphorylates p53 on Ser9 in vitro (Knippschild et al., 1997) and that p38 and casein kinase II phosphorylate p53 on Ser46 and Ser392, respectively, after UV radiation (Bulavin et al., 1999; Keller and Lu, 2002). It is reasonable to hypothesize that these kinases could phosphorylate the same p53 residues also in cells exposed to TMZ, thus contributing to stabilization and functional activation of the protein. The findings that p38α is activated in response to TMZ (Hirose et al., 2003) and that phosphorylation of p53 on Ser46, which, together with phosphorylation on Ser33, has been shown to be important for p53-induced apoptosis in response to UV (Bulavin et al., 1999), precedes PARP cleavage in both TMZ-treated TK6 and MT1 cells are consistent with this hypothesis.

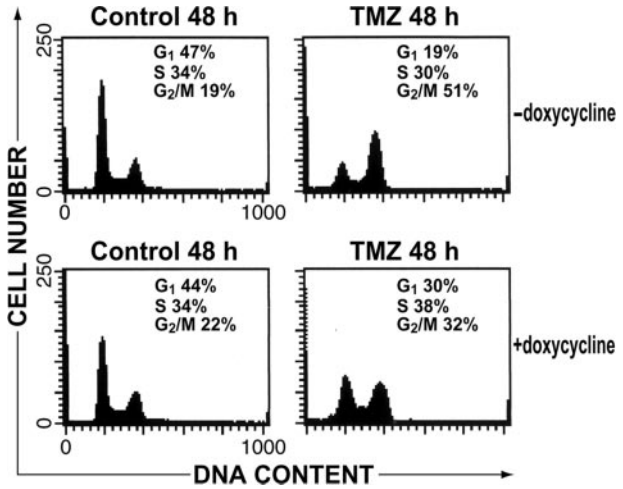

Fig. 9. Effect of ATR inhibition on G_2/M arrest induced by low TMZ concentrations. U2OS cells, stably transfected with a doxycycline-inducible ATR-kd expression construct, were cultured in the absence or in the presence of 1 μg/ml doxycycline for 24 h. BG (10 μM) and TMZ (25 μM) were then added to the cultures as described under *Materials and Methods*. Control groups were treated only with BG or doxycycline plus BG. Forty-eight hours after the addition of TMZ, the cells were harvested and processed for flow cytometric analysis of DNA content. The percentages of cells in the different phases of the cell cycle are indicated on each histogram. Similar results were obtained in two additional independent experiments.

In conclusion, the results obtained in this study provide further insights into the signal transduction pathways activated in response to methylating agents and the role played by the MMR system in their activation. Further studies will be necessary to better elucidate the mechanisms of ATM and ATR activation in TMZ-treated MMR- and MMR-deficient cells and to identify additional ATM and ATR downstream targets involved in cellular response to the drug.

Acknowledgments

We thank Dr. W. G. Thilly (MIT, Cambridge, MA) for providing the TK6 and MT1 cell lines, Dr. M. F. Lavin (The Queensland Cancer Fund Research Laboratory, Brisbane, Queensland, Australia) for providing the KT MAT1 and KT MEP cell lines, and Dr. P. Nghiem (Harvard University, Cambridge, MA) for providing the ATR-inducible U2OS cells. We also thank Maurizio Inzillo and Augusto Mari for the artwork and Dr. Federica Pochesci and Mauro Scarpellini for secretarial assistance.

References

Abraham RT (2001) Cell cycle checkpoint signaling through the ATM and ATR kinases. *Genes Dev* **15:**2177–2196.

Adamson AW, Kim WJ, Shangary S, Baskaran R, and Brown KD (2002) ATM is activated in response to *N*-methyl-*N*′-nitro-*N*-nitrosoguanidine-induced DNA alkylation. *J Biol Chem* **277:**38222–38229.

Bartek J, Falck J, and Lukas J (2001) CHK2 kinase—a busy messenger. *Nat Rev Mol Cell Biol* **2:**877–886.

Bertuzzi A, Gandolfi A, Germani A, and Vitelli R (1983) Estimation of cell DNA synthesis rate from flow-cytometric histograms. *Cell Biophys* **5:**223–236.

Brown KD, Rathi A, Kamath R, Beardsley DI, Zhan Q, Mannino JL, and Baskaran R (2003) The mismatch repair system is required for S-phase checkpoint activation. *Nat Genet* **33:**80–84.

Bulavin DV, Saito S, Hollander MC, Sakaguchi K, Anderson CW, Appella E, and Fornace AJ Jr (1999) Phosphorylation of human p53 by p38 kinase coordinates N-terminal phosphorylation and apoptosis in response to UV radiation. *EMBO (Eur Mol Biol Organ) J* **18:**6845–6854.

D'Atri S, Tentori L, Lacal PM, Graziani G, Pagani E, Benincasa E, Zambruno G, Bonmassar E, and Jiricny J (1998) Involvement of the mismatch repair system in temozolomide-induced apoptosis. *Mol Pharmacol* **54:**334–341.

Duckett DR, Bronstein SM, Taya Y, and Modrich P (1999) hMutSalpha- and hMutLalpha-dependent phosphorylation of p53 in response to DNA methylator damage. *Proc Natl Acad Sci USA* **96:**12384–12388.

Gatei M, Sloper K, Sorensen C, Syljuasen R, Falck J, Hobson K, Savage K, Lukas J, Zhou BB, Bartek J, et al. (2003) ATM and NBS1 dependent phosphorylation of CHK1 on S317 in response to IR. *J Biol Chem* **278:**14806–14811.

Gerson SL (2002) Clinical relevance of MGMT in the treatment of cancer. *J Clin Oncol* **20:**2388–2399.

Goldmacher VS, Cuzick RAJ, and Thilly WG (1986) Isolation and partial characterization of human cell mutants differing in sensitivity to killing and mutation by methylnitrosourea and *N*-methyl-*N*′-nitro-*N*-nitrosoguanidine. *J Biol Chem* **261:** 12462–12471.

Hickman MJ and Samson LD (1999) Role of DNA mismatch repair and p53 in signaling induction of apoptosis by alkylating agents. *Proc Natl Acad Sci USA* **96:**10764–10769.

Higashimoto Y, Saito S, Tong XH, Hong A, Sakaguchi K, Appella E, and Anderson CW (2000) Human p53 is phosphorylated on serines 6 and 9 in response to DNA damage-inducing agents. *J Biol Chem* **275:**23199–23203.

Hirao A, Kong YY, Matsuoka S, Wakeham A, Ruland J, Yoshida H, Liu D, Elledge SJ, and Mak TW (2000) DNA damage-induced activation of p53 by the checkpoint kinase Chk2. *Science (Wash DC)* **287:**1824–1827.

Hirose Y, Katayama M, Stokoe D, Haas-Kogan DA, Berger MS, and Pieper RO (2003) The p38 mitogen-activated protein kinase pathways links the DNA mismatch repair system to the G_2 checkpoint and to resistance to chemotherapeutic DNA-methylating agents. *Mol Cell Biol* **23:**8306–8315.

Jiricny J and Nyström-Lahti M (2000) Mismatch repair defects in cancer. *Curr Opin Genet Dev* **10:**157–161.

Kaina B, Ziouta A, Ochs K, and Coquerelle T (1997)Chromosomal instability, reproductive cell death and apoptosis induced by O^6-methylguanine in Mex^-, Mex^+ and

methylation-tolerant mismatch repair compromised cells: facts and models. *Mutat Res* **381:**227–241.
Karran P (2001) Mechanisms of tolerance to DNA damaging therapeutic drugs. *Carcinogenesis* **22:**931–1937.
Kat A, Thilly WG, Fang WH, Longley MJ, Li GM, and Modrich P (1993) An alkylation-tolerant, mutator human cell line is deficient in strand- specific mismatch repair. *Proc Natl Acad Sci USA* **90:**6424–6428.
Keller DM and Lu H (2002) p53 serine 392 phosphorylation increases after UV through induction of the assembly of the CK2.hSPT16.SSRP1 complex. *J Biol Chem* **277:**50206–50213.
Khanna KK, Lavin MF, Jackson SP, and Mulhern TD (2001) ATM, a central controller of cellular responses to DNA damage. *Cell Death Differ* **8:**1052–1065.
Knippschild U, Milne DM, Campbell LE, DeMaggio AJ, Christenson E, Hoekstra MF, and Meek DW (1997) p53 is phosphorylated *in vitro* and *in vivo* by the delta and epsilon isoforms of casein kinase 1 and enhances the level of casein kinase 1 delta in response to topoisomerase-directed drugs. *Oncogene* **15:** 1727–1736.
Liu Q, Guntuku S, Cui XS, Matsuoka S, Cortez D, Tamai K, Luo G, Carattini-Rivera S, DeMayo F, Bradley A, et al. (2000) Chk1 is an essential kinase that is regulated by Atr and required for the G_2/M DNA damage checkpoint. *Genes Dev* **14:**1448–1459.
Mirzoeva OK and Petrini JH (2001) DNA damage-dependent nuclear dynamics of the Mre11 complex. *Mol Cell Biol* **21:**281–288.
Modrich P (1997) Strand-specific mismatch repair in mammalian cells. *J Biol Chem* **272:**24727–24730.
Nghiem P, Park PK, Kim Y, Vaziri C, and Schreiber SL (2001) ATR inhibition selectively sensitize G_1 checkpoint-deficient cells to lethal premature chromatine condensation. *Proc Natl Acad Sci USA* **98:**9092–9097.
Papadopoulos N, Nicolaides NC, Liu B, Parsons R, Lengauer C, Palombo F, D'Arrigo A, Markowitz S, Willson JK, Kinzler KW, et al. (1995) Mutations of GTBP in genetically unstable cells. *Science (Wash DC)* **268:**1915–1917.
Pegg AE, Dolan ME, and Moschel RC (1995) Structure, function and inhibition of O6-alkylguanine-DNA alkyltransferase. *Prog Nucleic Acid Res Mol Biol* **51:**167–223.
Rhind N and Russell P (2000). Chk1 and Cds1: linchpins of the DNA damage and replication checkpoint pathways. *J Cell Sci* **113 (Pt 22):**3889–3896.
Saito S, Goodarzi AA, Higashimoto Y, Noda Y, Lees-Miller SP, Appella E, and Anderson CW (2002) ATM mediates phosphorylation at multiple p53 sites, including Ser^{46}, in response to ionizing radiation. *J Biol Chem* **277:**12491–12494.
Shiloh Y (2003) ATM and related protein kinases: safeguarding genome integrity. *Nat Rev Cancer* **3:**155–168.
Sionov RV and Haupt Y (1999) The cellular response to p53: the decision between life and death. *Oncogene* **18:**6145–6157.
Takai H, Naka K, Okada Y, Watanabe M, Harada N, Saito S, Anderson CW, Appella E, Nakanishi M, Suzuki H, et al. (2002) Chk2-deficient mice exhibit radioresistance and defective p53-mediated transcription. *EMBO (Eur Mol Biol Organ) J* **21:**5195–5205.
Taylor WR and Stark GR (2001) Regulation of the G2/M transition by p53. *Oncogene* **20:**1803–1815.
Ye R, Bodero A, Zhou BB, Khanna KK, Lavin MF, and Lees-Miller SP (2001) The plant isoflavenoid genistein activates p53 and Chk2 in an ATM-dependent manner. *J Biol Chem* **276:**4828–4833.
Zhang N, Chen P, Khanna KK, Scott S, Gatei M, Kozlov S, Watters D, Spring K, Yen T, and Lavin MF (1997) Isolation of full-length ATM cDNA and correction of the ataxia-telangiectasia cellular phenotype. *Proc Natl Acad Sci USA* **94:**8021–8026.
Zhao H and Piwnica-Worms H (2001) ATR-mediated checkpoint pathways regulate phosphorylation and activation of human Chk1. *Mol Cell Biol* **21:**4129–4139.
Zhou BB and Elledge SJ (2000) The DNA damage response: putting checkpoints in perspective. *Nature (Lond)* **408:**433–439.
Zhou XY, Wang X, Hu B, Guan J, Iliakis G, and Wang Y (2002) An ATM-independent S-phase checkpoint response involves CHK1 pathway. *Cancer Res* **62:**1598–1603.
Wang Y and Qin J (2003). MSH2 and ATR form a signalling module and regulate two branches of the damage response to DNA methylation. *Proc Natl Acad Sci USA* **100:**15387–92.

Address correspondence to: Stefania D'Atri, Istituto Dermopatico Dell'Immacolata (IDI-IRCCS), Via Monti di Creta 104, 00167 Rome, Italy. E-mail: s.datri@idi.it